Reversed interface effects in amorphous FeZr/AlZr multilayers

Martina Ahlberg,[*] Atieh Zamani, Erik Östman, Hossein Fashandi,[†] Björgvin Hjörvarsson, and Petra E. Jönsson
Department of Physics and Astronomy, Uppsala University, Box 516, SE-751 20 Uppsala, Sweden
(Received 29 November 2013; revised manuscript received 5 September 2014; published 4 November 2014)

We report an anomalous enhancement of the critical temperature (T_c) when the thickness (d) of the magnetic layer is decreased from 60 to 20 Å in amorphous FeZr/AlZr multilayers. Further reduction of the thickness causes a decrease of T_c, as expected by finite-size scaling, while the magnetic moment decreases monotonically for all values of d. The increase of the critical temperature is attributed to a reversed interface effect where local changes in the nearest-neighbor distance and coordination number gives a higher effective magnetic coupling at the interfaces compared to the interior of the layer. We have successfully described the results within a model where such interface effects are combined with finite-size scaling.

DOI: 10.1103/PhysRevB.90.184403 PACS number(s): 75.30.Kz, 75.50.Kj, 75.70.Cn

I. INTRODUCTION

Nanoscale materials are known to possess properties that can differ substantially from their bulk counterparts. Understanding the mechanisms behind those finite-size effects is essential to control and tailor the characteristics of materials. One fundamental property that changes with size is the magnetic ordering temperature (T_c), which is often stated to decrease as $T_c(d)/T_c(\infty) = 1 - c_0 d^{-\lambda}$, where d is the thickness and c_0 is a constant [1]. This expression has to be slightly modified to capture the behavior in the ultrathin-film limit [2,3]. The small adjustments do not change the overall trend and there is a basic understanding that T_c will decrease with decreasing thickness.

Opposite effects are found in thin iron films epitaxially grown on copper, where the critical temperature shows a maximum at a thickness of three monolayers [4,5]. Similar films deposited using pulsed laser deposition even show two maxima [6]. These unusual observations have been rationalized by linking structural transitions to the magnetic properties [7,8]. Exchange bias systems, where an antiferromagnetic thin film is coupled to a ferromagnet, also display an abnormal increase in T_c with decreasing thickness [9]. It is clear that there exist exceptions from the general rule that smaller extensions reduce T_c, but those examples are connected to structural changes or a close proximity to a bulk material with a high critical temperature.

Interactions at surfaces and interfaces are important parameters for the behavior of layered materials and nanoparticles [10–13]. Surfaces with stronger exchange coupling (J_s) than bulk (J_b) have been studied theoretically and the surface is predicted to order at a higher temperature compared to bulk when the ratio $J_s/J_b > 1.6$ [14]. This scenario is rarely observed [15,16] and the experimental difficulties are well illustrated by the example of Gd [17–19]. It was for long believed to have a separate surface ordering temperature, but a thorough study showed that the surface and bulk share the same T_c [19].

Intermixing at interfaces between magnetic and para- or nonmagnetic materials is known to lower the exchange coupling and gives rise to a lower T_c than expected from finite-size scaling [20,21]. In addition, interfaces play a key role for the performance of nanostructured devices [22] and it is therefore of vital importance to understand how they influence magnetic behavior.

Bulk FeZr has been a subject of basic research for decades, both due to its interesting properties [23–26] and as a model system for noncollinear magnetism [27,28]. In recent years, this material has been used to explore the thin-film physics of amorphous structures [29–32].

In this study, we address both interface effects and the thickness dependence of the critical temperature using iron-rich FeZr layers in FeZr/AlZr multilayers. We observe a reversed interface effect where the critical temperature *increases* with *decreasing* thickness, until a threshold value of $d \approx 20$ Å where T_c drops. The critical temperature is enhanced compared to the bulk even though there is no structural transition and the ferromagnetic layers are embedded in a paramagnetic material. We have successfully described the changes in the thin-film limit by a model where an increase of the effective magnetic coupling at the interfaces is combined with finite-size scaling.

II. EXPERIMENTAL DETAILS

A series of multilayers, together with a single film reference sample, were fabricated using dc magnetron sputtering following a recipe that has been successful in producing high quality amorphous layers [31,33]. The nominal structure of the multilayers were [FeZr(d)/AlZr(30 Å)]×10, where d = 15–60 Å, while the single FeZr film was 250 Å thick. The AlZr layers are thick enough to suppress any interlayer coupling between the magnetic layers [30]. The samples were grown on native oxide Si substrates, using 100 and 40 Å AlZr as buffer and capping layers, respectively. The single film was prepared using a thinner buffer layer of 30 Å. The notation of the samples in the paper is based on their nominal FeZr/AlZr thicknesses. The composition of the FeZr was estimated by comparing the critical temperature of the single film to other bulklike samples, giving an Fe content of $x \approx 92$ at.% [30,31,34,35]. The stoichiometry of the spacer layers is similar to the one determined for other samples produced using the same target, i.e., $Al_{75}Zr_{25}$ [32].

[*]Present address: Department of Physics, University of Gothenburg, SE-412 96 Göteborg, Sweden.
[†]Present address: Department of Physics, Chemistry and Biology, Linköping University, SE-581 83 Linköping, Sweden.

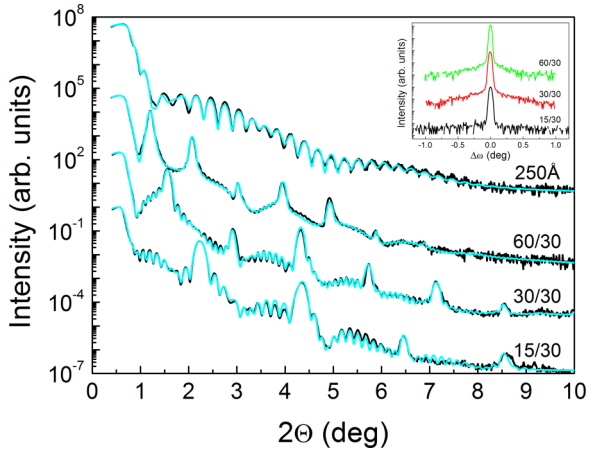

FIG. 1. (Color online) X-ray reflectivity data of four representative samples (black lines), together with the fits (cyan lines). (Inset) Transverse scans on the first-order multilayer peaks.

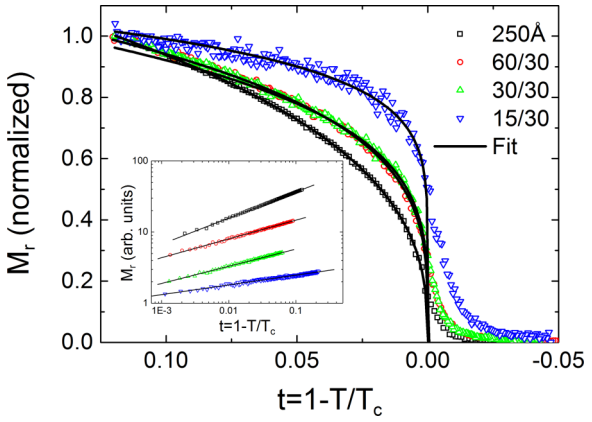

FIG. 2. (Color online) Normalized remanent magnetization vs the reduced temperature, together with fits. The inset shows the data and linear fits on a double logarithmic scale. Only the data points included in the fits are presented in the inset.

The structure of the multilayers was investigated using x-ray reflectivity (XRR) and the data was fitted using the GENX package [36]. Figure 1 shows representative examples of data together with the fits and the determined values of the FeZr layer thickness are listed in Table I. The roughness/intermixing of the layers was about 5 Å in all samples. The inset in Fig. 1 presents transverse scans on the first reflectivity peaks. The narrow width of the transverse peaks confirms a good layering in the samples.

The temperature dependence of the magnetization was measured using a setup utilizing the longitudinal magneto-optical Kerr effect (MOKE), for details see Ref. [37]. The critical temperature was determined by utilizing a well-known thermodynamic relationship, $M(t) \propto (t)^{\beta}$, where M is the spontaneous magnetization (M is commonly assumed to correspond to the remanent magnetization [38,39]), $t = 1 - T/T_c$ is the reduced temperature and β is a critical exponent [40]. The best fit of this expression to the remanent magnetization was found by varying T_c and the temperature range included in the fit [37]. Figure 2 shows examples of experimental data together with the fits on both linear and double logarithmic scales. The results are found in Fig. 3 and Table I.

TABLE I. Results of the analysis of the XRR, MOKE, and SQUID data. The magnetic moment was determined in a field of 4 T and at a temperature of $0.5T_c$. The 250-Å sample was not completely saturated at this field.

Sample	d_{FeZr} (Å)	T_c (K)	β	δ	μ (μ_B/Fe)
15/30	14.1(2)	154.8(9)	0.14(3)	8.5(1)	1.04(11)
20/30	20.8(3)	195.7(9)	0.18(3)	9.4(4)	1.33(10)
25/30	25.9(2)	192.0(9)	0.20(3)	10.6(1.1)	–
30/30	32.5(3)	187.7(9)	0.24(3)	10.8(1.8)	1.41(12)
40/30	43.1(1)	182.0(9)	0.28(3)	10.5(2.1)	–
50/30	53.1(1)	177.9(9)	0.26(3)	8.3(2)	–
60/30	61.9(4)	174.8(9)	0.26(3)	8.9(6)	1.54(8)
250 Å	253(1)	172.6(9)	0.37(3)	5.8(6)	1.15(3)

The magnetic moment of selected samples was extracted from the magnetic response in fields ranging from 0.2 to 4 T, measured by a SQUID magnetometer (Quantum Design MPMS). The moment as a function of the FeZr layer thickness is plotted in Fig. 3 and listed in Table I. The measurements were made at $0.5T_c$, which is above the transverse-spin-freezing temperature [41]. It is easier to saturate the samples at these temperatures, reducing the need of very high fields. The determined moment can thus not be directly compared to literature values, which are commonly measured at 5 K, but the general trend of the moment increasing with Fe content is still valid. The lower μ of the 250-Å film is due to a prominent noncollinear effect and the applied field was too low to reach saturation.

III. RESULTS AND DISCUSSION

The values of the exponent β are consistent with a dimensional crossover from 2D to 3D behavior [42], but one exponent is not enough to verify that a sample belong

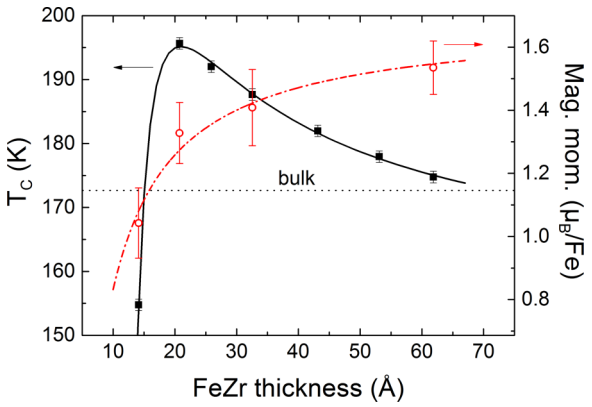

FIG. 3. (Color online) The critical temperature (solid squares) and magnetic moment (open circles) as a function of the FeZr layer thickness. The bulk (250 Å) values of both properties are represented by the dotted horizontal line. The black solid line and the red dash-dotted line represents fits to Eq. (2) and Eq. (3), respectively.

to a certain universality class. We therefore also determined the exponent δ ($M(H,T_c) \propto H^{1/\delta}$), using a field range of 0.2–6.5 mT. None of the δ values matched the class implied by β. We can thus not confirm a dimensional crossover. The data support the finding that systems where disorder is linked to magnetic canting and frustration cannot be characterized by a single set of exponents [43].

The critical temperature shows an unusual dependence on the FeZr layer thickness (d). It contradicts the predictions of finite-size scaling and *increases* with *decreasing* thickness. A similar trend has been observed in an exchange bias system where antiferromagnetic thin films of different thicknesses are coupled to a bulklike high T_c ferromagnet [9]. In the model used to explain the behavior, the Néel temperature diverges for very thin layers [10], while in this study, the critical temperature shows a rapid decline below a maximum at $d = 20$ Å. Moreover, the magnetic layers are not in contact with another thick ferromagnetic layer. Therefore we need a new model to describe the present observations.

The critical temperature and the magnetic moment of Fe_xZr_{100-x} are strongly dependent on the Fe concentration and both increase up to a threshold value of about $x \approx 85$ [44–48]. Above this concentration, T_c decreases and measurements using high fields (up to 11 T) show an increase of the as determined μ [49]. The reduction of T_c at high concentrations is commonly attributed to a decrease of the distance between iron atoms [50,51] and an increase in Fe-Fe coordination number [52,53].

Interfaces between two amorphous materials cannot have any atomic steps and for the same reason they can never be "atomically" flat. In the region between FeZr and AlZr, the coordination number and the Fe-Fe distance change continuously and the local magnetic moment, anisotropy, and the exchange coupling must therefore be different from bulk. The result of these modifications will only be evident when J increases at the interface given that the opposite condition easily is interpreted as a common consequence of intermixing. Furthermore, since the influence of the interfaces is more significant for thinner films the effect will increase with decreasing thickness.

In addition to the effects observed in the thickness range of 20–60 Å, one must bear in mind the inherent decrease in T_c that is expected for thin films [1–3]. Zhang and Willis have successfully described the reduction of the critical temperature in crystalline materials by dividing the thickness dependence into two segments. The initial decline follows a power law and crosses over to a linear behavior in the ultrathin limit [3]. In their stated relationship, the thickness is expressed in monolayers (ML) and it implies that $T_c = 0$ K at 1 ML. Therefore we need to make small adjustments of the equations, to take into account that ferromagnetic order vanishes in amorphous layers with thicknesses in the range of 5–11 Å [31,54], giving

$$\frac{T_c(d)}{T_c(\infty)} = \begin{cases} 1 - [(N_0 + a)/2(d - d_0)]^{\lambda} & (d > N_0 + d_0) \\ (d - d_0)/2N_0 & (d < N_0 + d_0) \end{cases}, \quad (1)$$

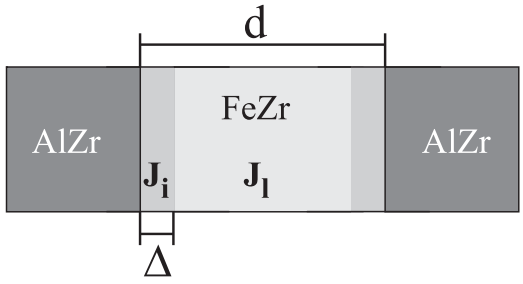

FIG. 4. A schematic image of the structure of the multilayer samples. d is the thickness of the FeZr layers and Δ is the spatial extension of the interface region with modified magnetic parameters compared to bulk. The average exchange interactions in the interior of the layer and at the interface are denoted J_l and J_i, respectively.

where d is the film thickness, d_0 is the thickness where no magnetic order appears above $T > 0$ K, N_0 is the range of spin-spin interactions, λ is a shift exponent, and a is a constant corresponding to the thickness of one monolayer in the crystalline case. The interpretation of the constant a is ambiguous for amorphous materials, but its value should be in the range of 1–3 Å. Here, we use crystalline iron as a reference and set $a = 1.44$ Å.

To validate the hypothesis that the changes in T_c and μ are caused by changes in local magnetic parameters at the interface, we employed a mean-field model and postulate that the critical temperature is proportional to the exchange coupling, $T_c \propto J$. We further assumed that the reduction of T_c is reflected in the magnetic coupling of the whole sample and attain the following expression:

$$J_{\text{eff}}(d) = [2\Delta J_i(d) + (d - 2\Delta)J_l(d)]/d, \quad (2)$$

where Δ is the spatial extension of the interface, and J_i and J_l are the exchange couplings of the interface and the interior of the layer, respectively. $J_i(d)$ and $J_l(d)$ are described by Eq. (1). The parameters are also illustrated in Fig. 4.

The fit of Eq. (2) to the data is shown in Fig. 3 and it captures the observed behavior very well in the thin-film limit. The bulk critical temperature is underestimated, but this is reasonable considering that no thickness dependencies of the magnetic frustration or interatomic distances are taken into account. The parameters $\lambda = 1.6$, $N_0 = 3.2$ Å [3], and $\Delta = 5$ Å (given by the XRR results) were fixed during the fit, in order to reduce the degrees of freedom and since Δ and J_i are strongly interdependent. The best fit gave $d_0 = 9.7$ Å, $J_i = 271$ K, and $J_l = 158$ K. The J values reveal a substantial increase of the magnetic interactions at the interfaces which might be surprising considering the relatively low Zr content of the spacer, but it is important to note that the critical temperature of $Fe_{90}Zr_{10}$ increases when Fe is substituted with Al [55]. The limiting thickness d_0 is often interpreted in terms of magnetically "dead" layers [21]. That description fails in the present context, since the interfaces are very much "alive." Instead the chemical and topological medium range order has to be considered to elucidate this point, i.e., the consequences of the layer thickness approaching the length scales where amorphous materials appear structurally ordered [56,57].

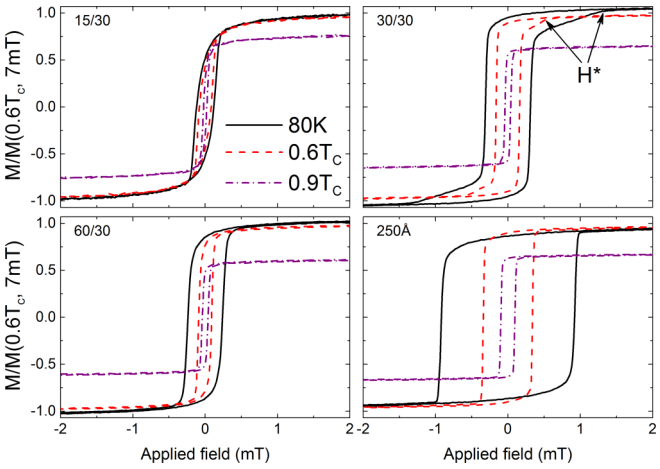

FIG. 5. (Color online) Hysteresis curves measured at 80 K, $0.6T_c$, and $0.9T_c$. The loops are normalized to the signal at $T = 0.6T_c$ and $\mu_0 H_{max} = 7$ mT. The closing field (H^*) where the upper and lower branches of the hysteresis loop meet is marked out in the top right figure.

The magnetization as a function of d is described within the same model as $T_c(d)$ by the following expression:

$$\mu(d) = [2\Delta\mu_i + (d - 2\Delta)\mu_l]/d. \quad (3)$$

Again two values are strongly dependent, but in this fit Δ was used as a free parameter and the ratio μ_i/μ_l was considered to be equal to $J_l/J_i = 0.58$ (i.e., a linear relationship between μ and T_c). The fit is presented in Fig. 3 and the deduced values are $\mu_l = 1.7\mu_B$ and $\Delta = 6.0$ Å.

The significant impact of the modified magnetic properties at the interface is corroborated by the shape of the hysteresis curves, which differs between the samples, both at absolute and relative temperatures (Fig. 5). While the thicker FeZr layers show a clear isotropic response, signs of a hard switching emerge as the layer thickness decreases and reveals the coupling between the bulk and the interfaces. The situation is reminiscent of exchange spring multilayers consisting of hard and soft magnetic materials [58,59], but here the hard phase is merely an interface. The anisotropic feature can be quantified by defining a closing field (H^*) where the upper and lower branches of the hysteresis loop meet, see Fig. 5. The result is shown in Fig. 6, where the different coercive fields (H_c) are taken into account by plotting the difference between H^* and H_c. The similarity between the evolution of H^* and the critical temperature is striking. The strong interactions at the interface alter the behavior of sufficiently thin layers, while the properties of thick films are governed by the bulk. The thinnest layers (14.1 Å) consists effectively of two merged interfaces and the very narrow hysteresis loops together with the low remanence show that they are on the verge of the critical thickness where no ferromagnetic order is observed.

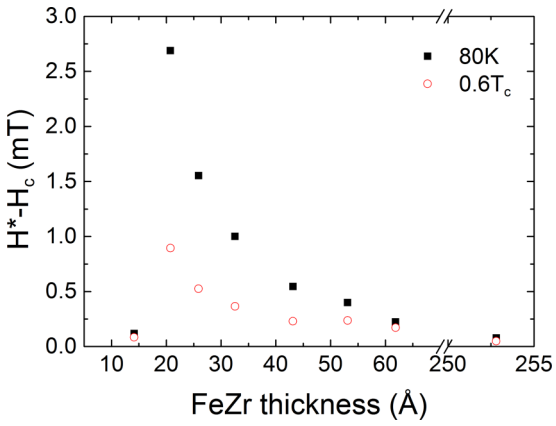

FIG. 6. (Color online) The closing field (H^*) subtracted by the coercive field (H_c) vs the FeZr layer thickness. Note the broken x axis.

The coercivity is highest for the thickest 250-Å sample. Bulk FeZr is a noncollinear ferromagnet and H_c increases with Fe content due to magnetic frustration, mainly in the plane perpendicular to the applied field [60]. Thin films are more collinear due to demagnetization effects and hence the coercivity decreases in the ultrahin limit.

The effects presented here are not expected to be limited to iron-rich FeZr, nor to low temperatures. Amorphous FeB, for example, display a similar maximum in T_c with concentration, but the highest critical temperature is around 600 K [61]. The presence of other elements than Zr (or B) can also increase the magnetic coupling at the interface. This is already obvious for the case of Al in this study and is supported by results showing that incorporation of carbon in FeZr increase T_c with up to 120% [62].

IV. CONCLUSIONS

We have demonstrated a reversed interface effect which locally gives rise to an enhanced magnetic coupling compared to bulk. This leads to an increase of the critical temperature with decreasing layer thickness, in opposite to the expected decrease. We have described the results by a mean field model that successfully captures the behavior in the thin-film limit. The findings open for new routes to stabilize the magnetic properties of small structures by proper engineering of the interfaces.

ACKNOWLEDGMENTS

The authors acknowledge financial support from the Swedish Research Council (Vetenskapsrådet), Knut and Alice Wallenberg foundation and the Göran Gustafsson Foundation. We thank Vassilios Kapaklis for helpful discussions.

[1] G. A. T. Allan, Phys. Rev. B **1**, 352 (1970).
[2] F. Huang, G. J. Mankey, M. T. Kief, and R. F. Willis, J. Appl. Phys. **73**, 6760 (1993).
[3] R. Zhang and R. F. Willis, Phys. Rev. Lett. **86**, 2665 (2001).
[4] M. Stampanoni, Appl. Phys. A **49**, 449 (1989).
[5] J. Thomassen, F. May, B. Feldmann, M. Wuttig, and H. Ibach, Phys. Rev. Lett. **69**, 3831 (1992).
[6] H. Jenniches, J. Shen, C. V. Mohan, S. S. Manoharan, J. Barthel, P. Ohresser, M. Klaua, and J. Kirschner, Phys. Rev. B **59**, 1196 (1999).

[7] M. Zharnikov, A. Dittschar, W. Kuch, C. M. Schneider, and J. Kirschner, Phys. Rev. Lett. **76**, 4620 (1996).
[8] A. Biedermann, Phys. Rev. B **80**, 235403 (2009).
[9] P. J. van der Zaag, Y. Ijiri, J. A. Borchers, L. F. Feiner, R. M. Wolf, J. M. Gaines, R. W. Erwin, and M. A. Verheijen, Phys. Rev. Lett. **84**, 6102 (2000).
[10] X. Y. Lang, W. T. Zheng, and Q. Jiang, Phys. Rev. B **73**, 224444 (2006).
[11] H. Zabel, J. Phys. Condens. Matter **11**, 9303 (1999).
[12] A. Razouk, M. Sahlaoui, and M. Sajieddine, J. Supercond. Novel Magn. **24**, 2019 (2011).
[13] C. Waldfried, T. McAvoy, D. Welipitiya, P. A. Dowben, and E. Vescovo, Europhys. Lett. **42**, 685 (1998).
[14] K. Binder and D. P. Landau, Phys. Rev. Lett. **52**, 318 (1984).
[15] M. Pleimling, J. Phys. A: Math. Gen **37**, R79 (2004).
[16] A. Enders, R. Skomski, and J. Honolka, J. Phys.: Condens. Matter **22**, 433001 (2010).
[17] D. Weller, S. F. Alvarado, W. Gudat, K. Schröder, and M. Campagna, Phys. Rev. Lett. **54**, 1555 (1985).
[18] E. D. Tober, F. J. Palomares, R. X. Ynzunza, R. Denecke, J. Morais, Z. Wang, G. Bino, J. Liesegang, Z. Hussain, and C. S. Fadley, Phys. Rev. Lett. **81**, 2360 (1998).
[19] C. S. Arnold and D. P. Pappas, Phys. Rev. Lett. **85**, 5202 (2000).
[20] Y.-H. Liu, X.-D. Ma, and L.-M. Mei, Phys. Rev. B **45**, 10459 (1992).
[21] S.-K. Kim, J.-R. Jeong, J. B. Kortright, and S.-C. Shin, Phys. Rev. B **64**, 052406 (2001).
[22] C. A. F. Vaz, J. A. C. Bland, and G. Lauhoff, Rep. Prog. Phys. **71**, 056501 (2008).
[23] H. Hiroyoshi and K. Fukamichi, J. Appl. Phys. **53**, 2226 (1982).
[24] Z. Altounian and J. O. Strom-Olsen, Phys. Rev. B **27**, 4149 (1983).
[25] V. A. Makarov and A. S. Kozlova, Sov. Phys. JETP **72**, 461 (1991).
[26] K. Balakrishnan, P. Babu, V. Ganesan, R. Srinivasan, and S. N. Kaul, J. Magn. Magn. Mater **250**, 110 (2002).
[27] I. Bakonyi, Acta Mater. **53**, 2509 (2005).
[28] R. Lorenz and J. Hafner, J. Magn. Magn. Mater **139**, 209 (1995).
[29] P. Sharma, H. Kimura, and A. Inoue, Phys. Rev. B **78**, 134414 (2008).
[30] A. Liebig, P. T. Korelis, M. Ahlberg, and B. Hjörvarsson, Phys. Rev. B **84**, 024430 (2011).
[31] P. T. Korelis, P. E. Jönsson, A. Liebig, H. E. Wannberg, P. Nordblad, and B. Hjörvarsson, Phys. Rev. B **85**, 214430 (2012).
[32] V. Kapaklis, G. K. Pálsson, J. Vegelius, M. M. Haverhals, P. T. Korelis, S. M. Butorin, A. Modin, M. Kavčič, M. Žitnik, K. Bučar, K. O. Kvashnina, and B. Hjörvarsson, J. Phys. Condens. Matter **24**, 495402 (2012).
[33] P. T. Korelis, A. Liebig, M. Björck, B. Hjörvarsson, H. Lidbaum, K. Leifer, and A. R. Wildes, Thin Solid Films **519**, 404 (2010).
[34] V. Kapaklis, P. T. Korelis, B. Hjörvarsson, A. Vlachos, I. Galanakis, P. Poulopoulos, K. Özdoğan, M. Angelakeris, F. Wilhelm, and A. Rogalev, Phys. Rev. B **84**, 024411 (2011).
[35] A. Zamani, A. Hallén, P. Nordblad, G. Andersson, B. Hjörvarsson, and P. E. Jönsson, J. Magn. Magn. Mater. **346**, 138 (2013).
[36] M. Björck and G. Andersson, J. Appl. Crystallogr. **40**, 1174 (2007).
[37] M. Ahlberg, P. Korelis, G. Andersson, and B. Hjörvarsson, Phys. Rev. B **85**, 224425 (2012).
[38] C. Back, C. Würsch, A. Vaterlaus, U. Ramsperger, U. Maier, and D. Pescia, Nature (London) **378**, 597 (1995).
[39] T. S. Bramfeld and R. F. Willis, J. Appl. Phys. **103**, 07C718 (2008).
[40] H. E. Stanley, *Introduction to Phase Transitions and Critical Phenomena* (Oxford University Press, Oxford, 1993).
[41] D. H. Ryan, J. M. Cadogan, and J. van Lierop, Phys. Rev. B **61**, 6816 (2000).
[42] T. S. Bramfeld, H. Won, and R. F. Willis, J. Appl. Phys. **107**, 09E150 (2010).
[43] C. M. Haetinger, L. Ghivelder, J. Schaf, and P. Pureur, J. Phys. Condens. Matter **21**, 506006 (2009).
[44] F. J. Castaño, T. Stobiecki, M. R. J. Gibbs, M. Czapkiewicz, M. Kopcewicz, V. Gacem, J. Speakman, N. Cowlam, and H. J. Blythe, J. Phys. Condens. Matter **9**, 10603 (1997).
[45] K. Fukamichi and R. J. Gambino, IEEE Trans. Magn. **17**, 3059 (1981).
[46] J. M. D. Coey, D. H. Ryan, and Y. Boliang, J. Appl. Phys. **55**, 1800 (1984).
[47] N. Heiman and N. Kazama, Phys. Rev. B **19**, 1623 (1979).
[48] K. Shirakawa, K. Fukamichi, T. Kaneko, and T. Masumoto, Physica B+C **119**, 192 (1983).
[49] K. M. Unruh and C. L. Chien, Phys. Rev. B **30**, 4968 (1984).
[50] D. H. Ryan and J. M. Cadogan, J. Magn. Magn. Mater. **213**, 111 (2000).
[51] X. Qian and W. Hübner, Phys. Rev. B **67**, 184414 (2003).
[52] Y. Kakehashi, T. Uchida, and M. Yu, Phys. Rev. B **56**, 8807 (1997).
[53] M. Yu and Y. Kakehashi, J. Magn. Magn. Mater **162**, 189 (1996).
[54] M. Ahlberg, G. Andersson, and B. Hjörvarsson, Phys. Rev. B **83**, 224404 (2011).
[55] U. Carow-Watamura, D. V. Louzguine, and A. Takeuchi, Al-Fe-Zr (058), in *SpringerMaterials - The Landolt-Börnstein Database*, edited by Y. Kawazoe, U. Carow-Watamura, and J. Z. Yu (Springer-Verlag, Berlin Heidelberg, 2011).
[56] A. P. Sokolov, A. Kisliuk, M. Soltwisch, and D. Quitmann, Phys. Rev. Lett. **69**, 1540 (1992).
[57] A. Hirata, P. Guan, T. Fujita, Y. Hirotsu, A. Inoue, A. R. Yavari, T. Sakurai, and M. Chen, Nat. Mater. **10**, 28 (2011).
[58] E. E. Fullerton, J. S. Jiang, C. H. Sowers, J. E. Pearson, and S. D. Bader, Appl. Phys. Lett. **72**, 380 (1998).
[59] R. Skomski, J. Phys.: Condens. Matter **15**, R841 (2003).
[60] D. H. Ryan, J. M. D. Coey, E. Batalla, Z. Altounian, and J. O. Ström-Olsen, Phys. Rev. B **35**, 8630 (1987).
[61] J. Kamarád and Z. Arnold, Physica B+C **139-140**, 382 (1986).
[62] R. Moubah, A. Zamani, A. Olsson, S. Shi, A. Hallen, S. Carlson, D. Arvanitis, P. Nordblad, B. Hjörvarsson, and P. Jönsson, Appl. Phys. Express **6**, 053001 (2013).